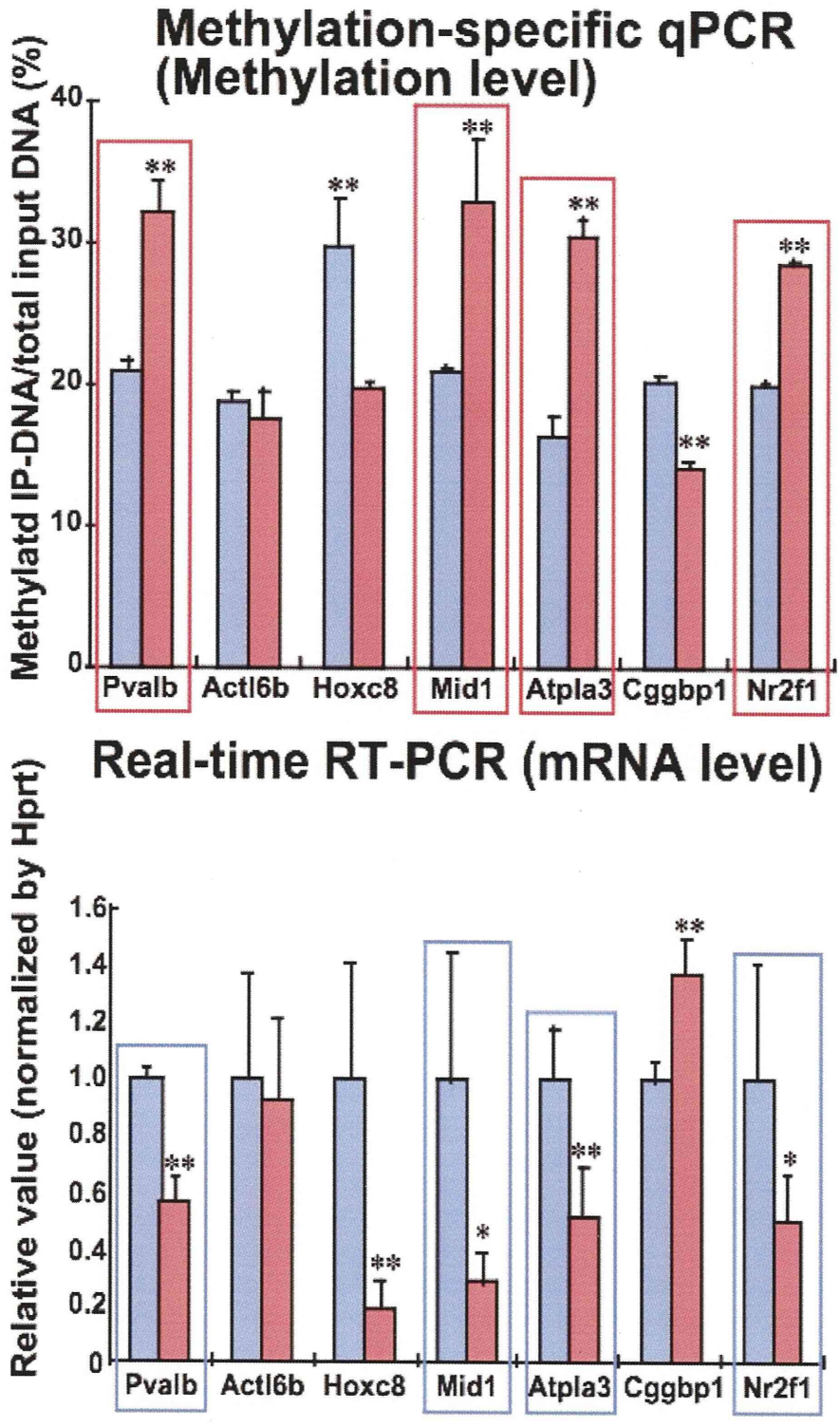

Fig. 23. Methylation-specific qPCR analysis and real-time RT-PCR analysis of male offspring at PND 21 after maternal exposure to $MnCl_2 \cdot 4H_2O$ from GD 10 to PND 21 in mice.

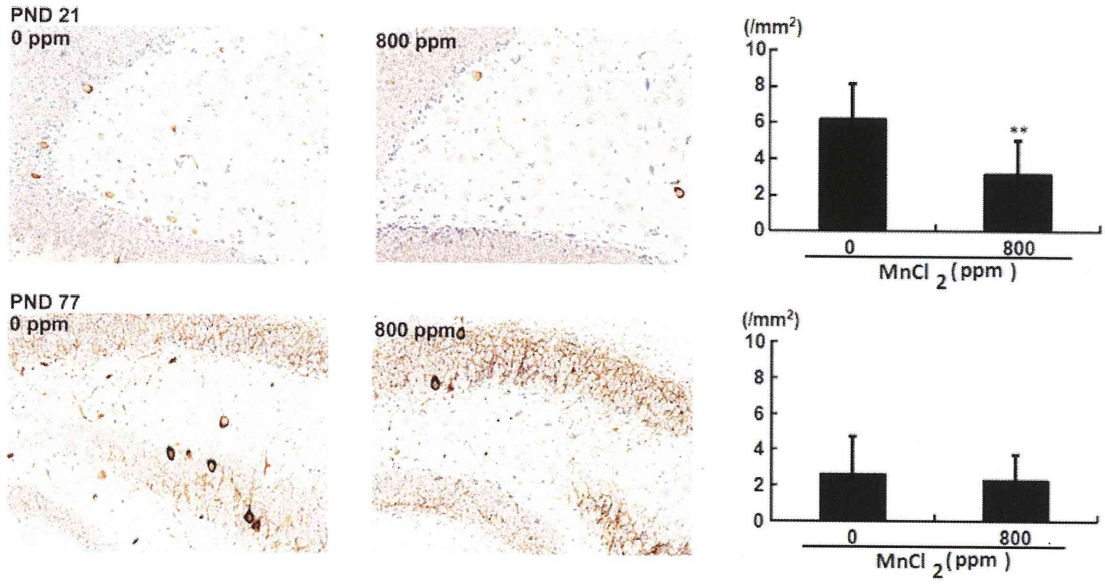

Fig. 24. Distribution of Parvalbmin-immunoreactive cells in the dentate hilus of male offspring at PND 21 and 77 after maternal exposure to $MnCl_2 \cdot 4H_2O$ from GD 10 to PND 21 in mice.

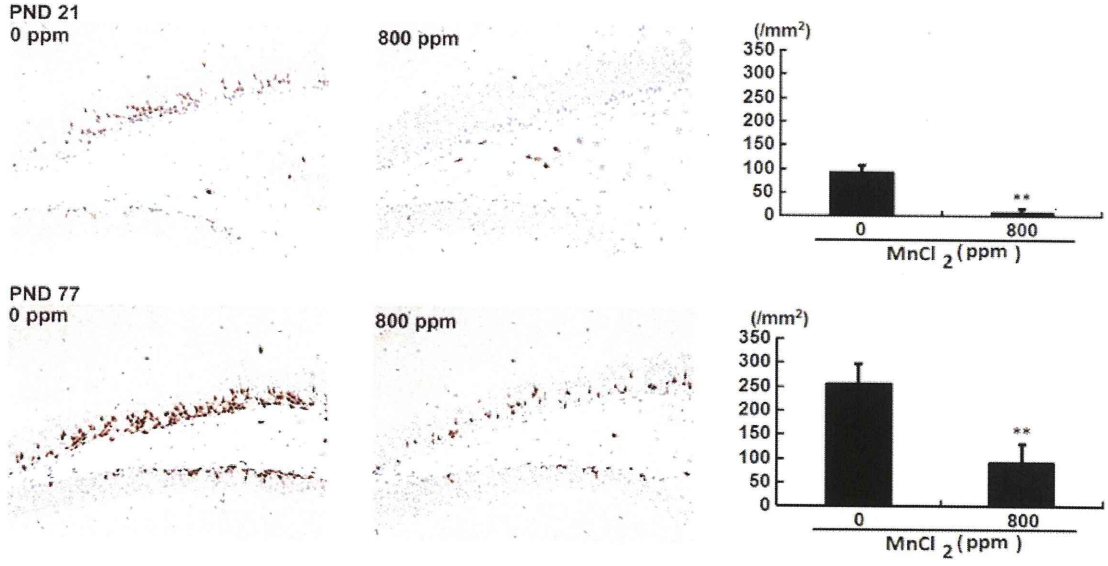

Fig. 25. Distribution of MID1-immunoreactive cells in the dentate hilus of male offspring at PND 21 and 77 after maternal exposure to $MnCl_2 \cdot 4H_2O$ from GD 10 to PND 21 in mice.

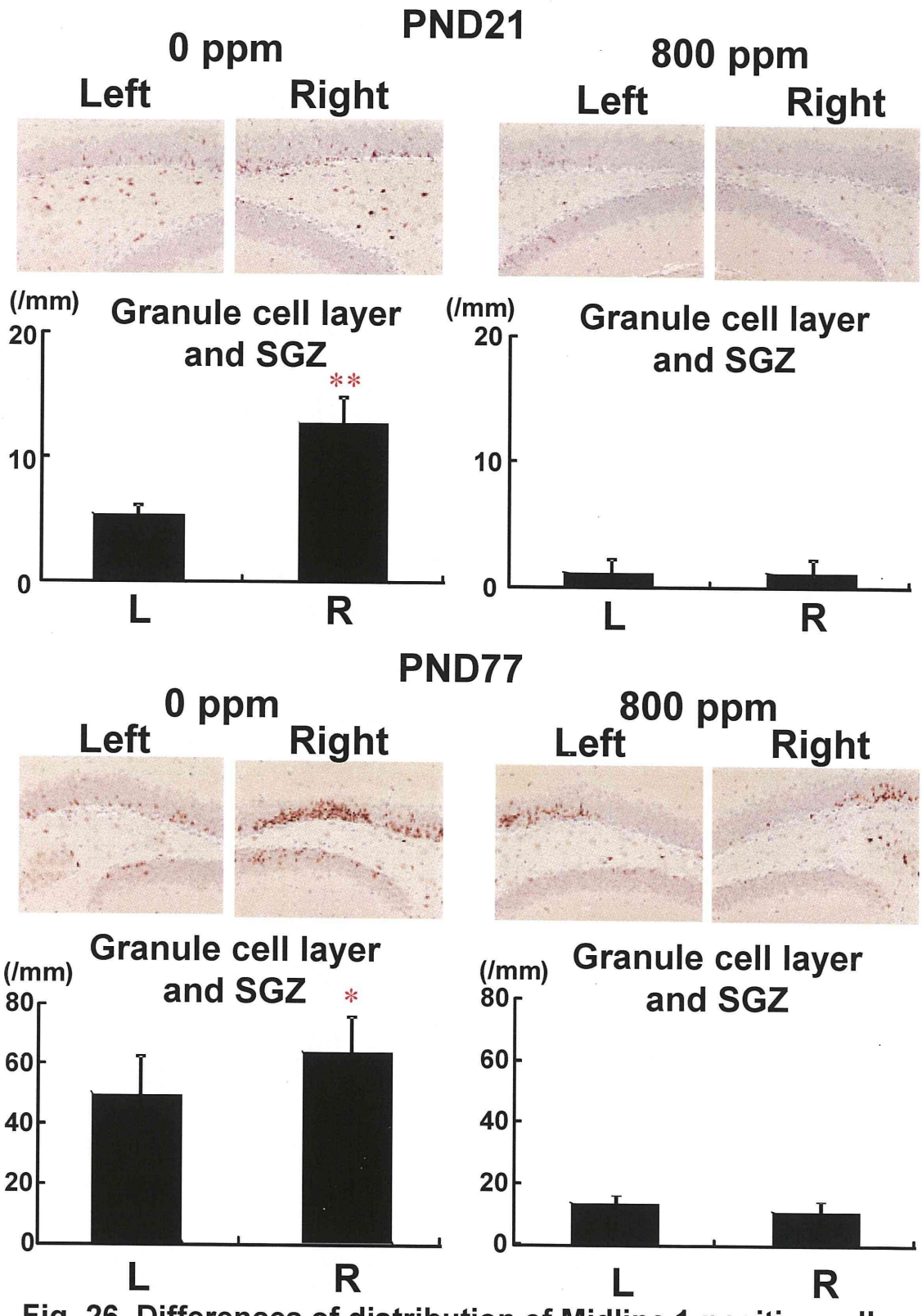

Fig. 26. Differences of distribution of Midline 1-positive cells between right and left side in the dentate subgranular zone of male offspring at PND 21 and 77 after maternal exposure to $MnCl_2 \cdot 4H_2O$ from GD 10 to PND 21 in mice.

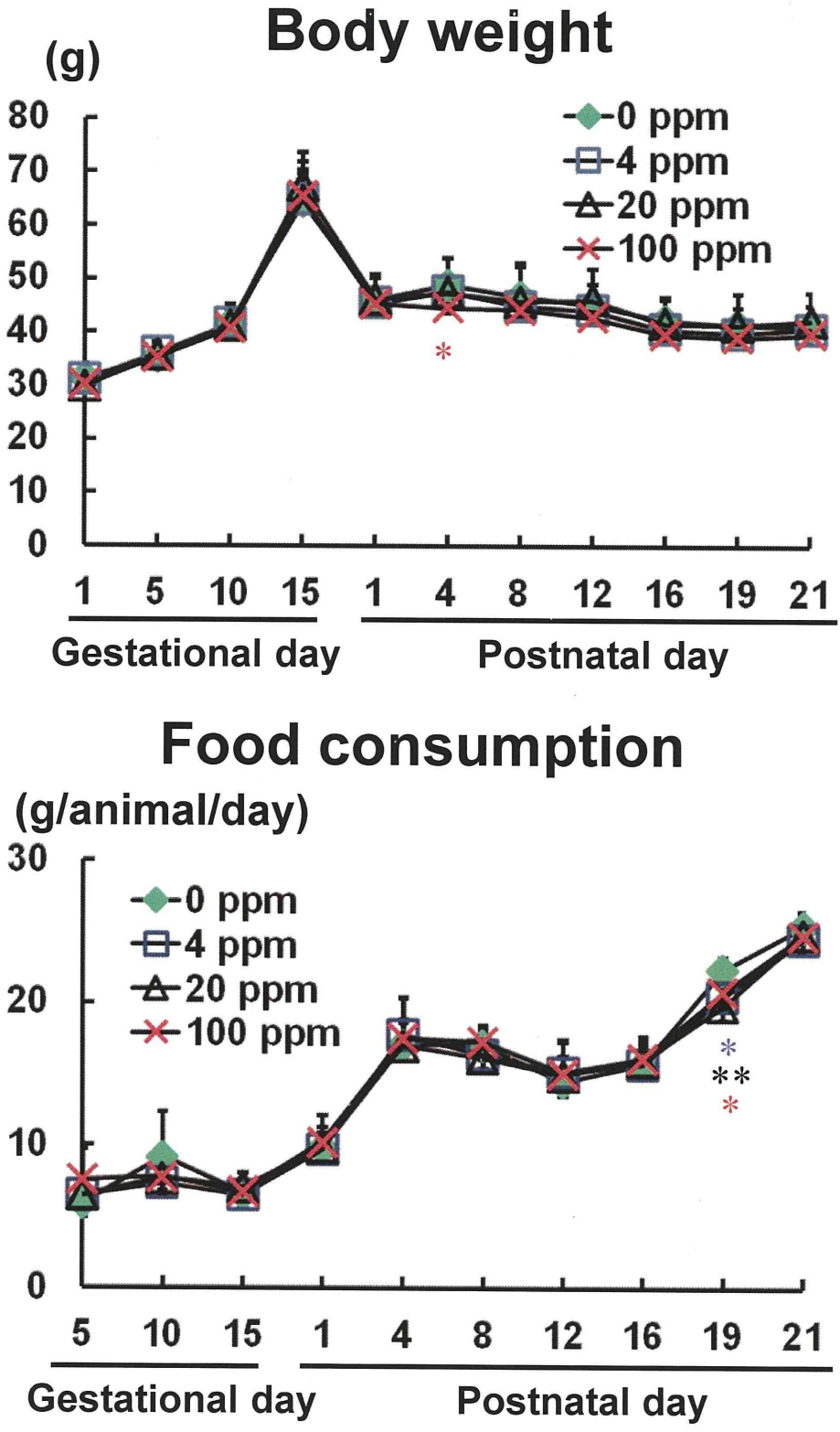

Fig. 27. Body weights and food consumption of dams exposed to chlorpyryfos from GD 10 to PND 21 in mice.

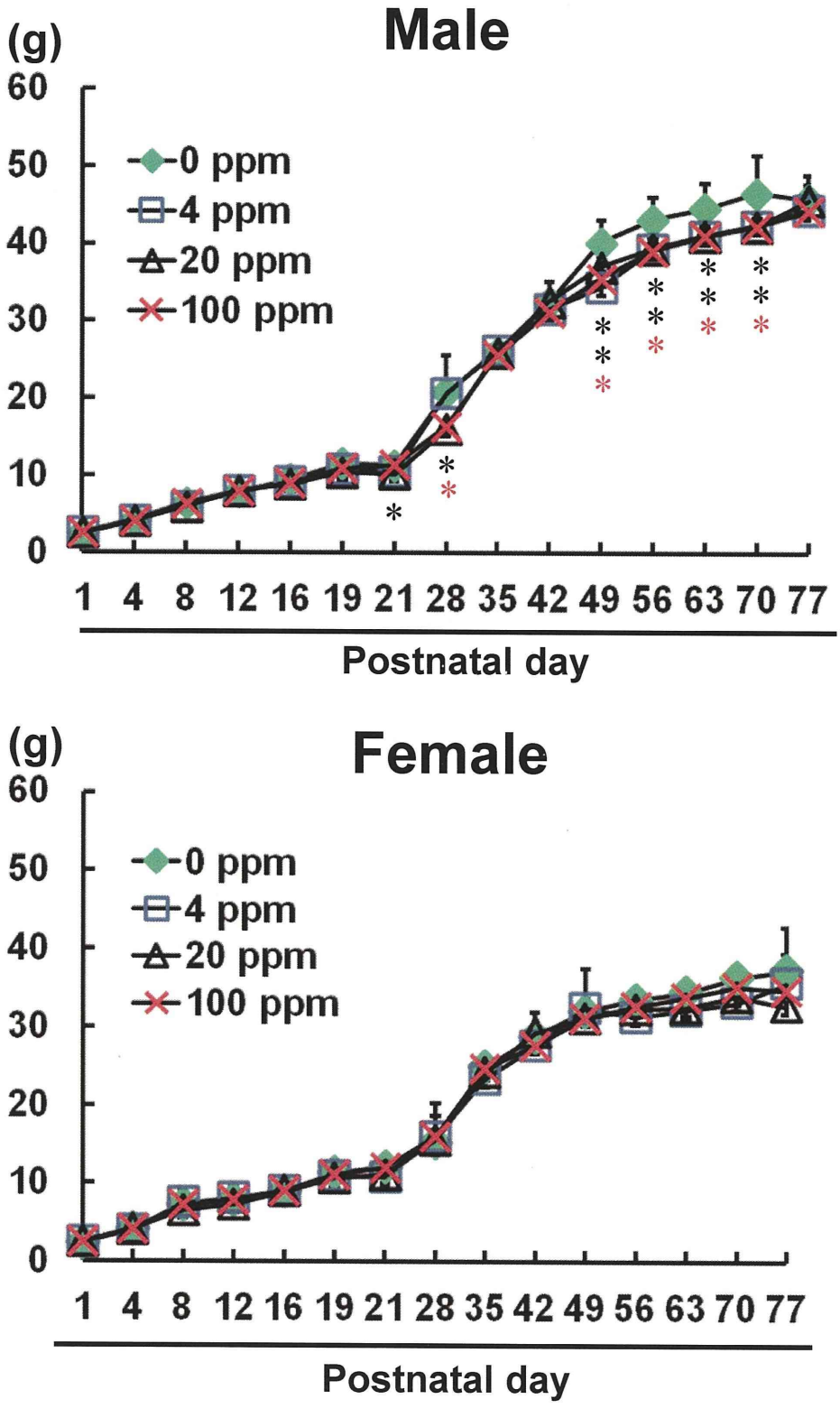

Fig. 28. Body weights of offspring after maternal exposure to chlorpyryfos from GD 10 to PND 21 in mice.

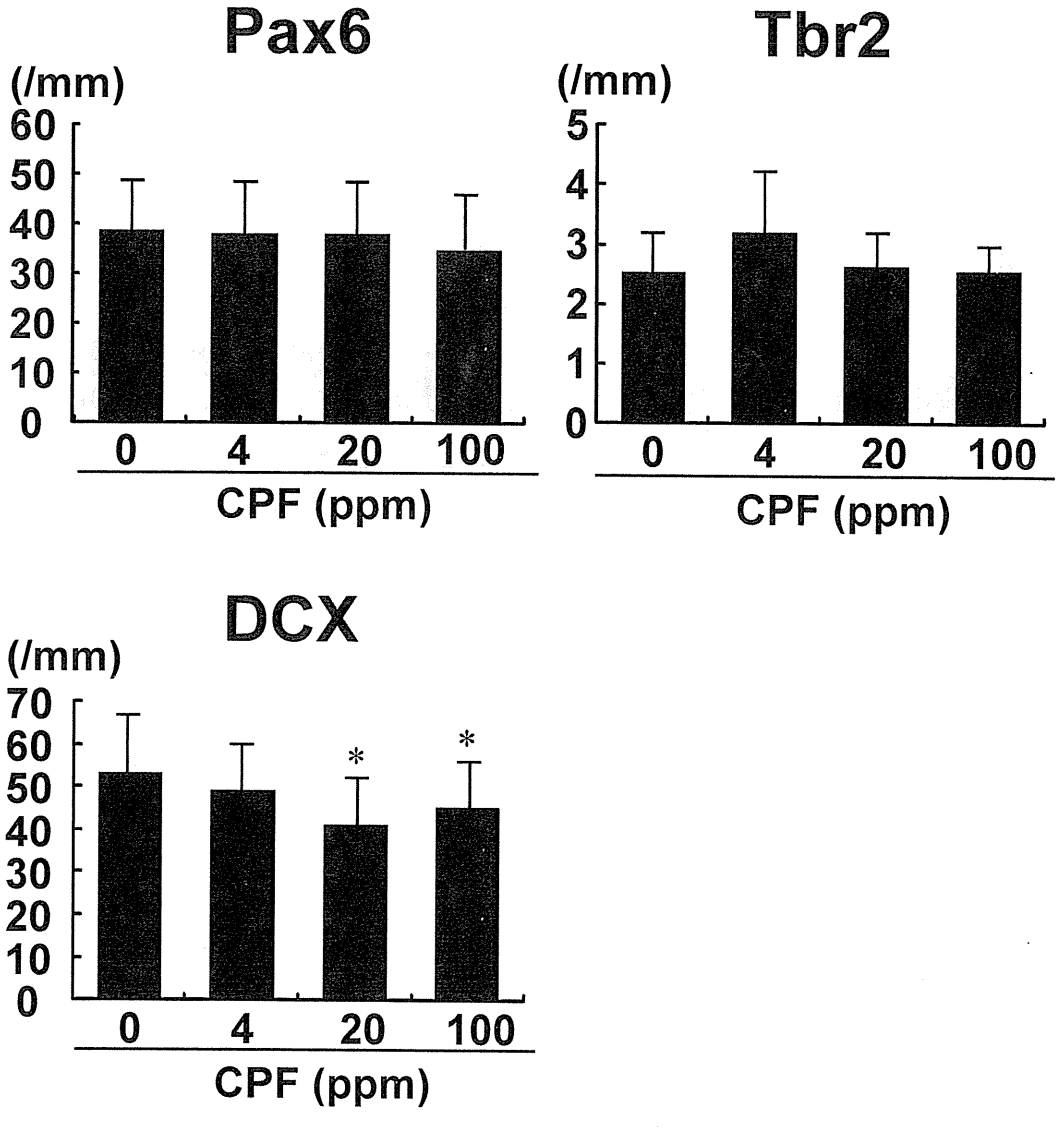

Fig. 29. Distribution of Pax6, Tbr2 and DCX-positive cells in the dentate subgranular zone of male offspring at PND 21 after maternal exposure to chlorpyrifos from GD 10 to PND 21 in mice.

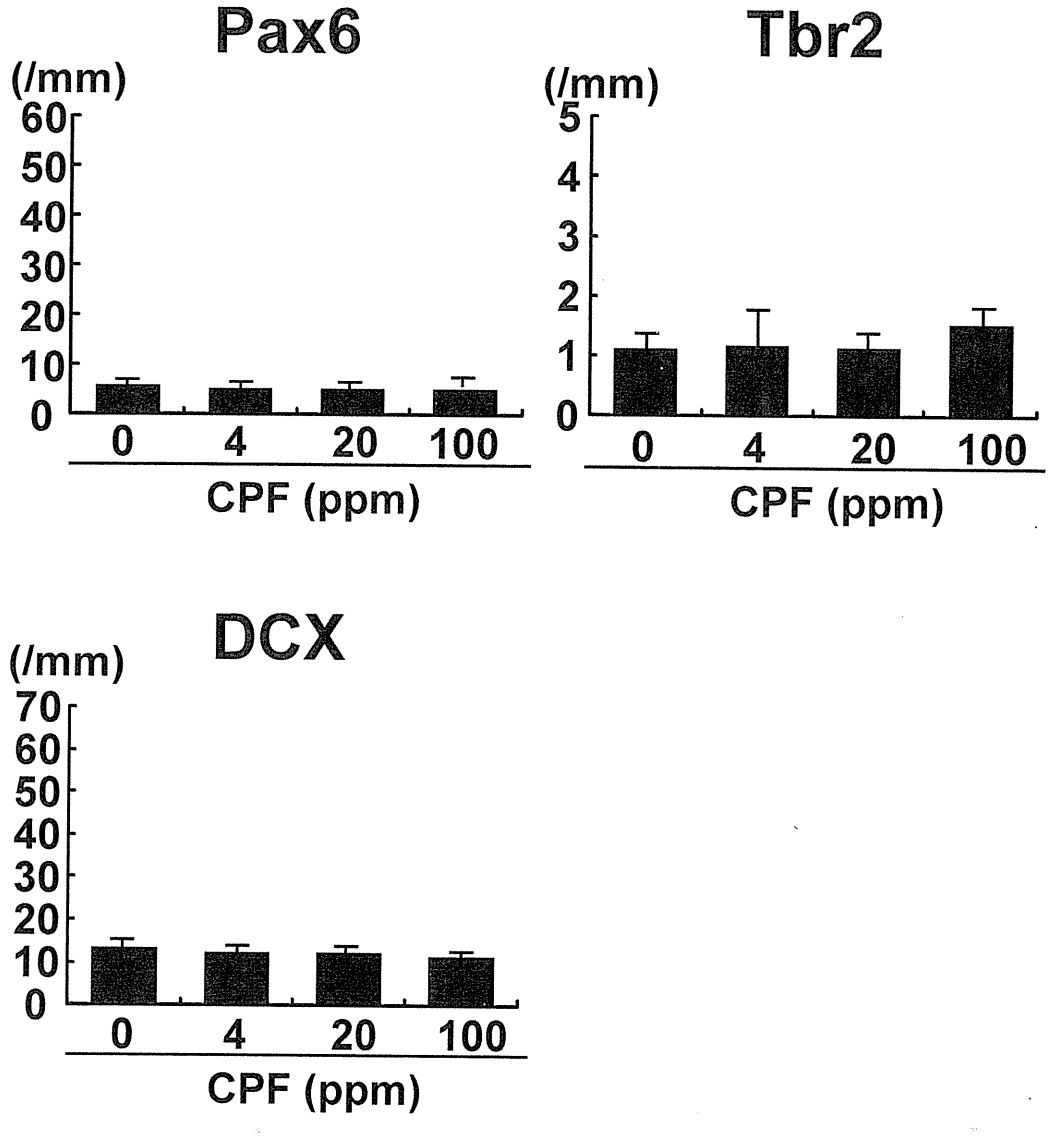

Fig. 30. Distribution of Pax6, Tbr2 and DCX-positive cells in the dentate subgranular zone of male offspring at PND 77 after maternal exposure to chlorpyrifos from GD 10 to PND 21 in mice.

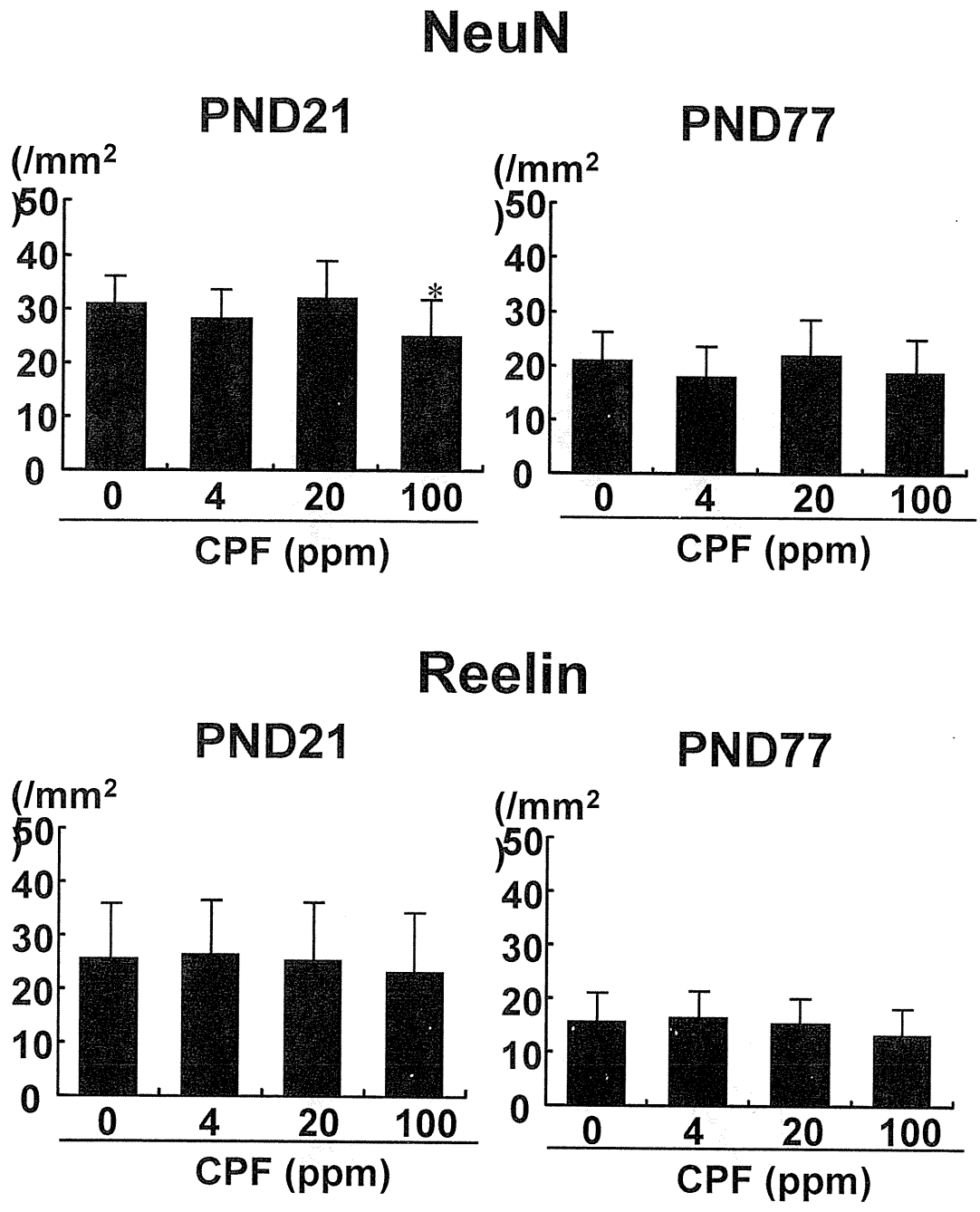

Fig. 31. Distribution of NeuN and Reelin-positive cells in the dentate subgranular zone of male offspring at PND 21 and 77 after maternal exposure to chlorpyrifos from GD 10 to PND 21 in mice.

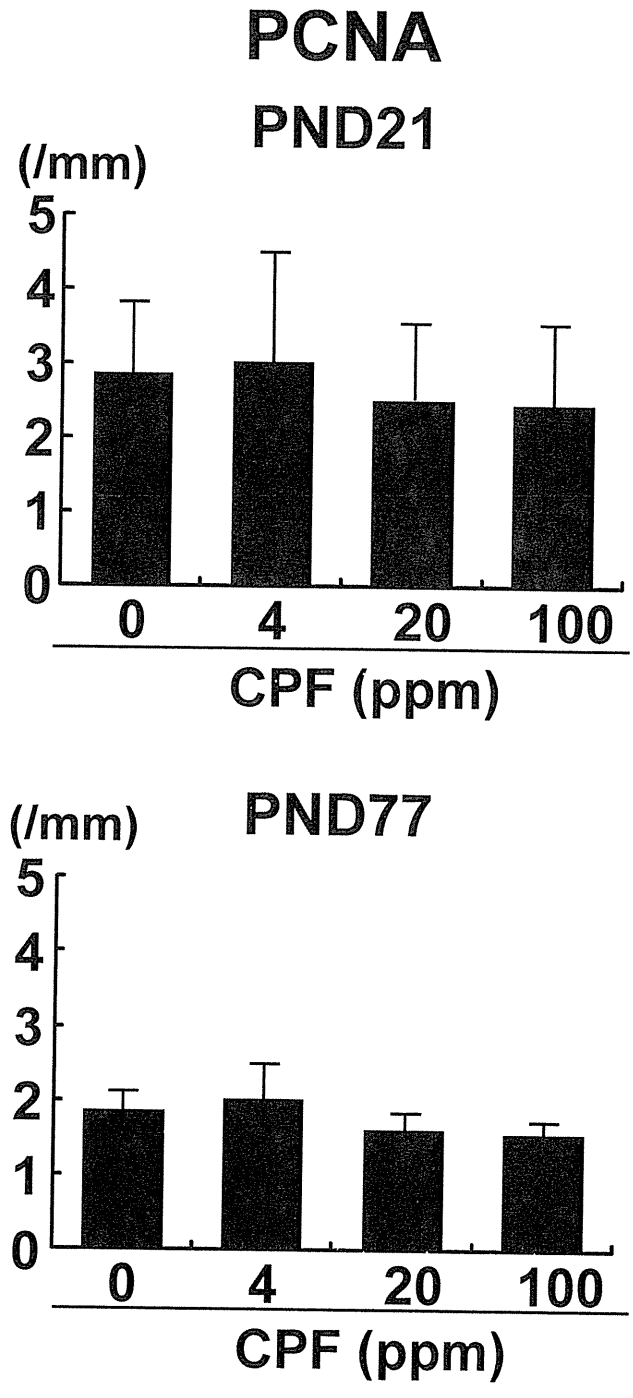

Fig. 32. Distribution of PCNA-positive cells in the dentate subgranular zone of male offspring at PND 21 and 77 after maternal exposure to chlorpyrifos from GD 10 to PND 21 in mice.

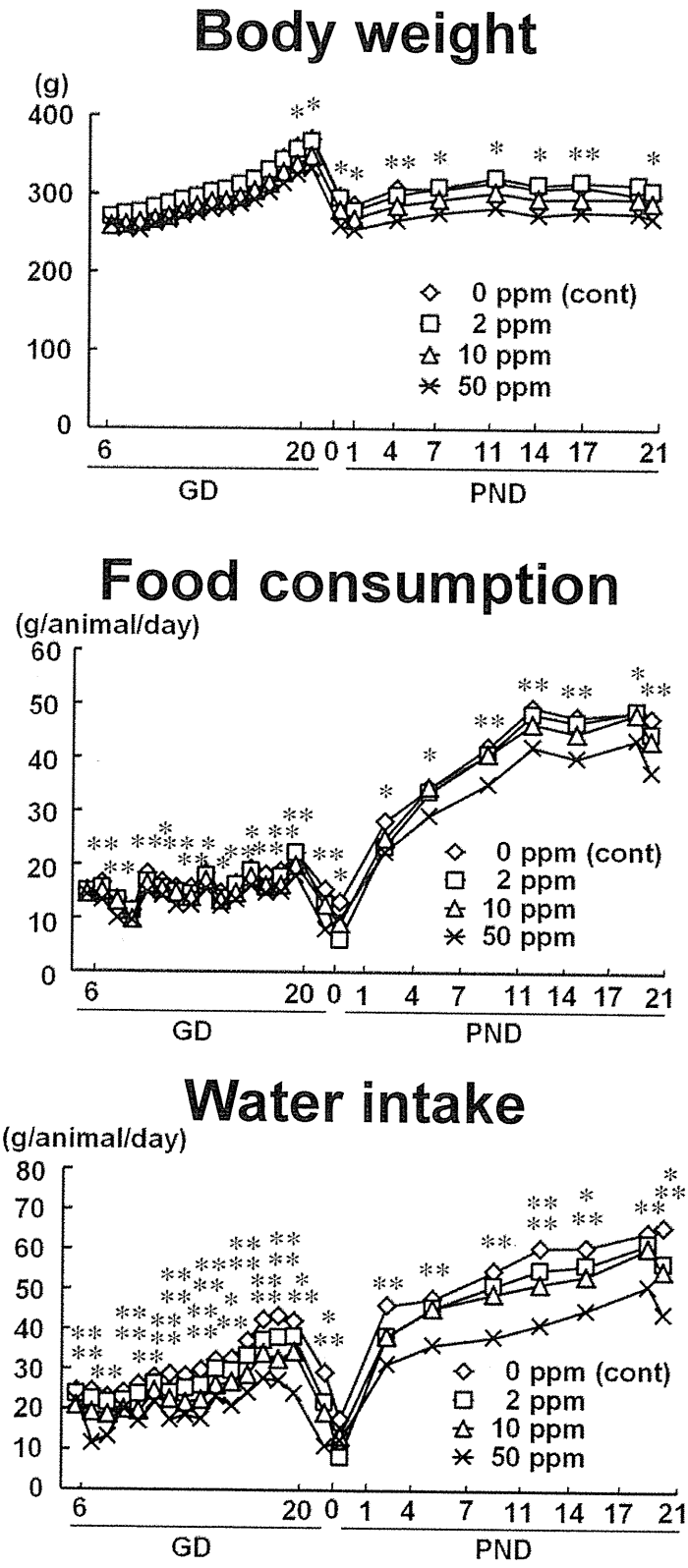

Fig. 33. Body weights, food consumption and water intake of dams exposed to nicotine hydrogen tartrate salt from GD 6 to PND 21 in rats.

Body weight

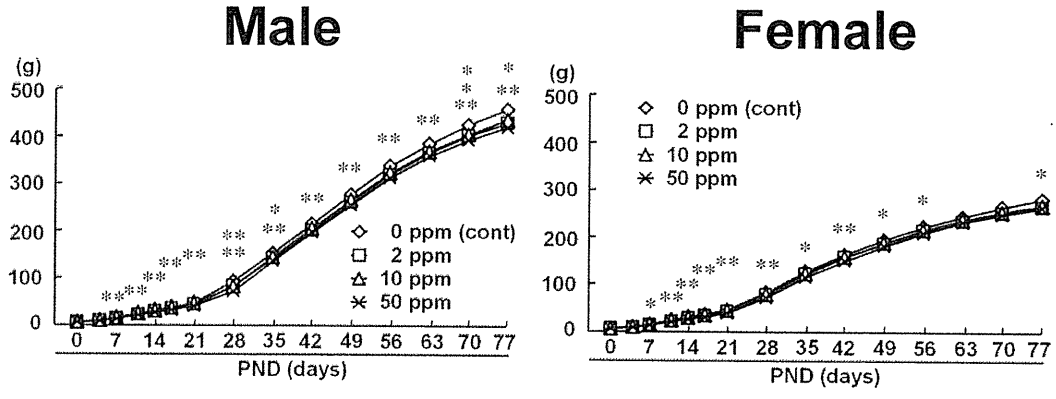

Food consumption

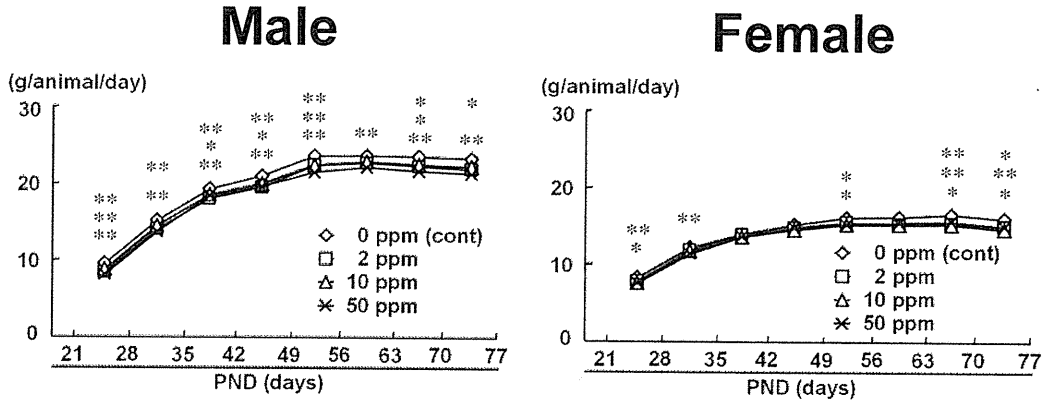

Fig. 34. Body weights and food consumption of offspring after maternal exposure to nicotine hydrogen tartrate salt from GD 6 to PND 21 in rats.

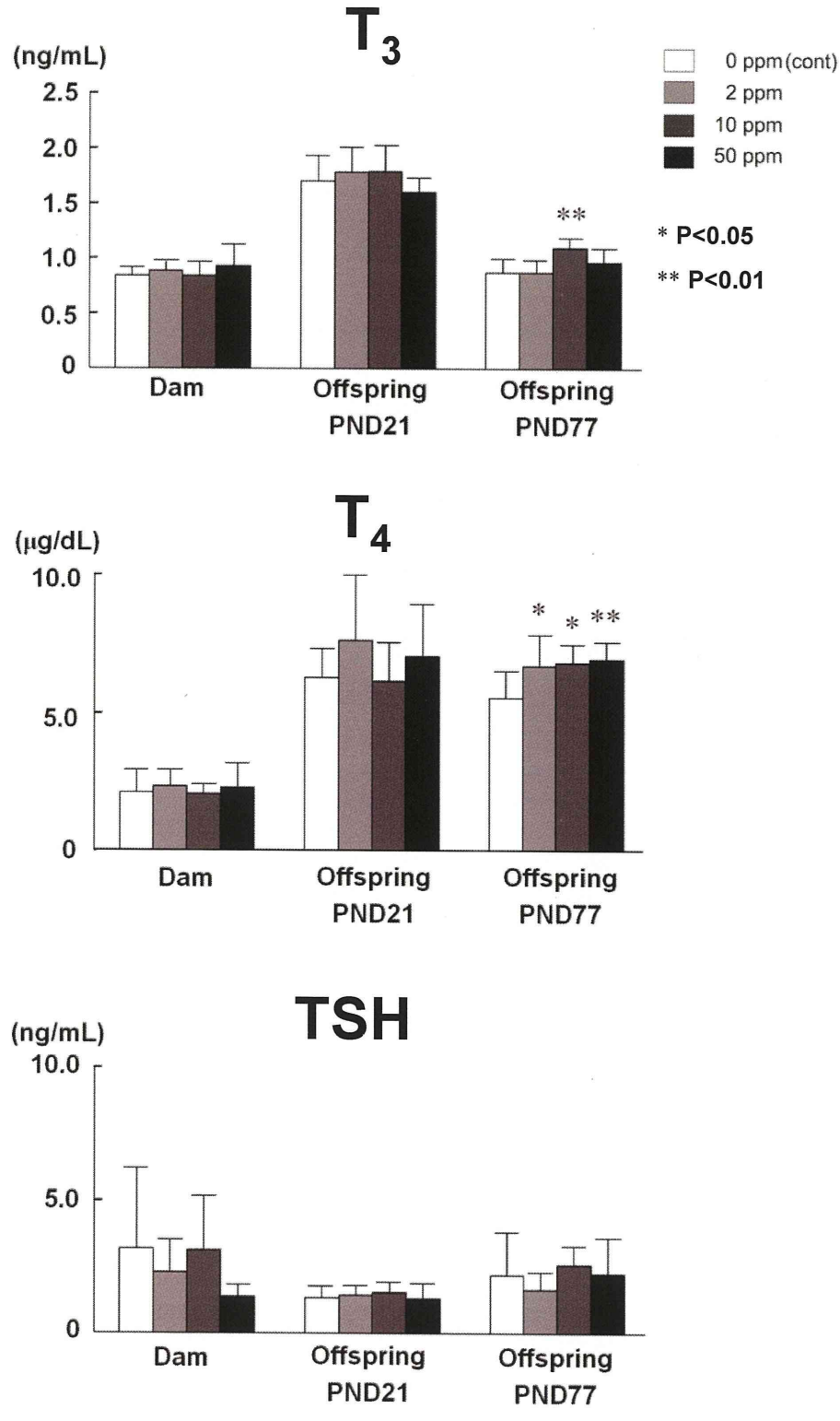

Fig. 35. Thyroid related-hormones of male offspring and dams exposed to nicotine hydrogen tartrate salt from GD 6 to PND 21 in rats.

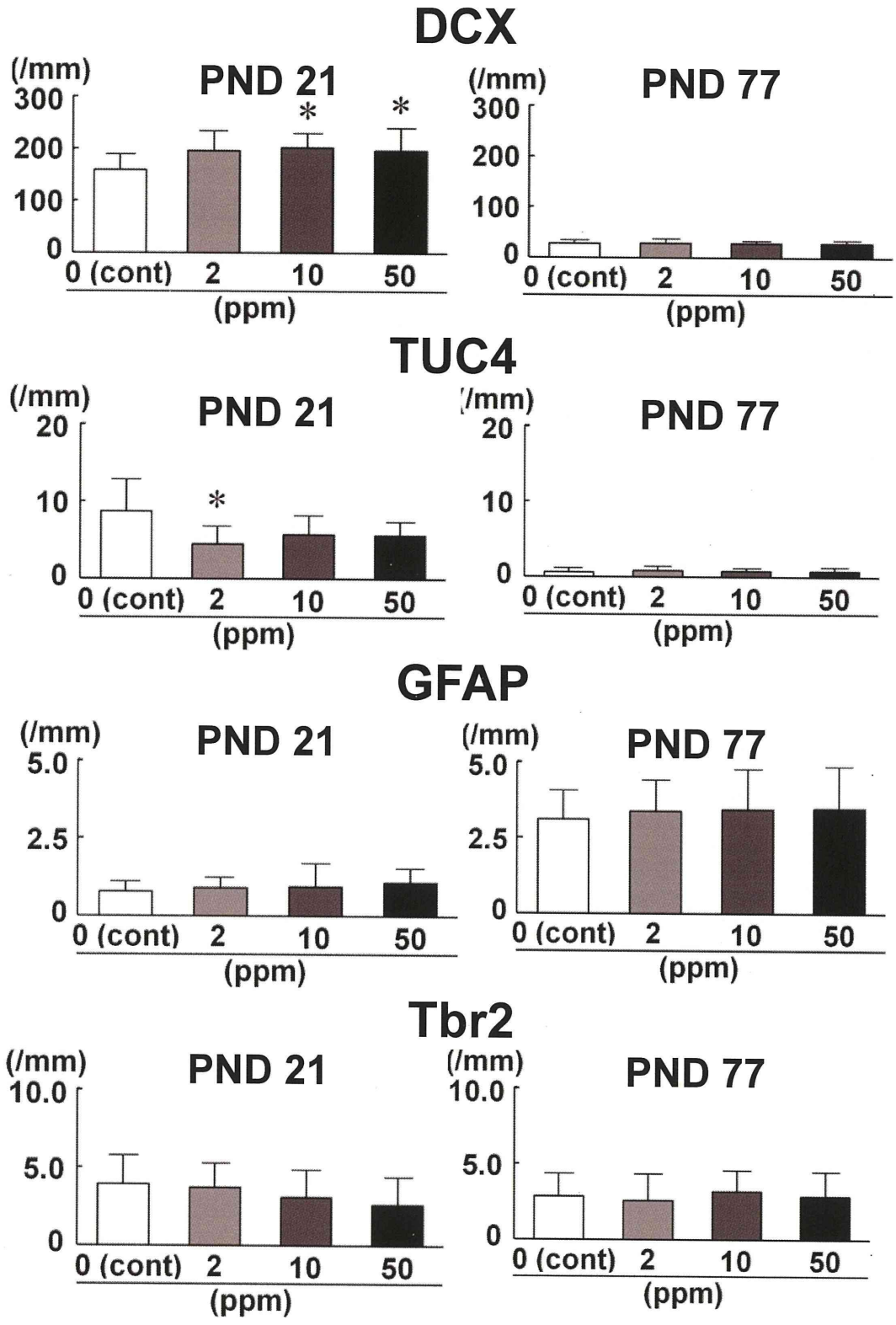

Fig. 36. Distribution of DCX, TUC4, GFAP and Tbr2 -positive cells in the dentate subgranular zone of male offspring at PND 21 and 77 after maternal exposure to nicotine hydrogen tartrate salt from GD 6 to PND 21 in rats.

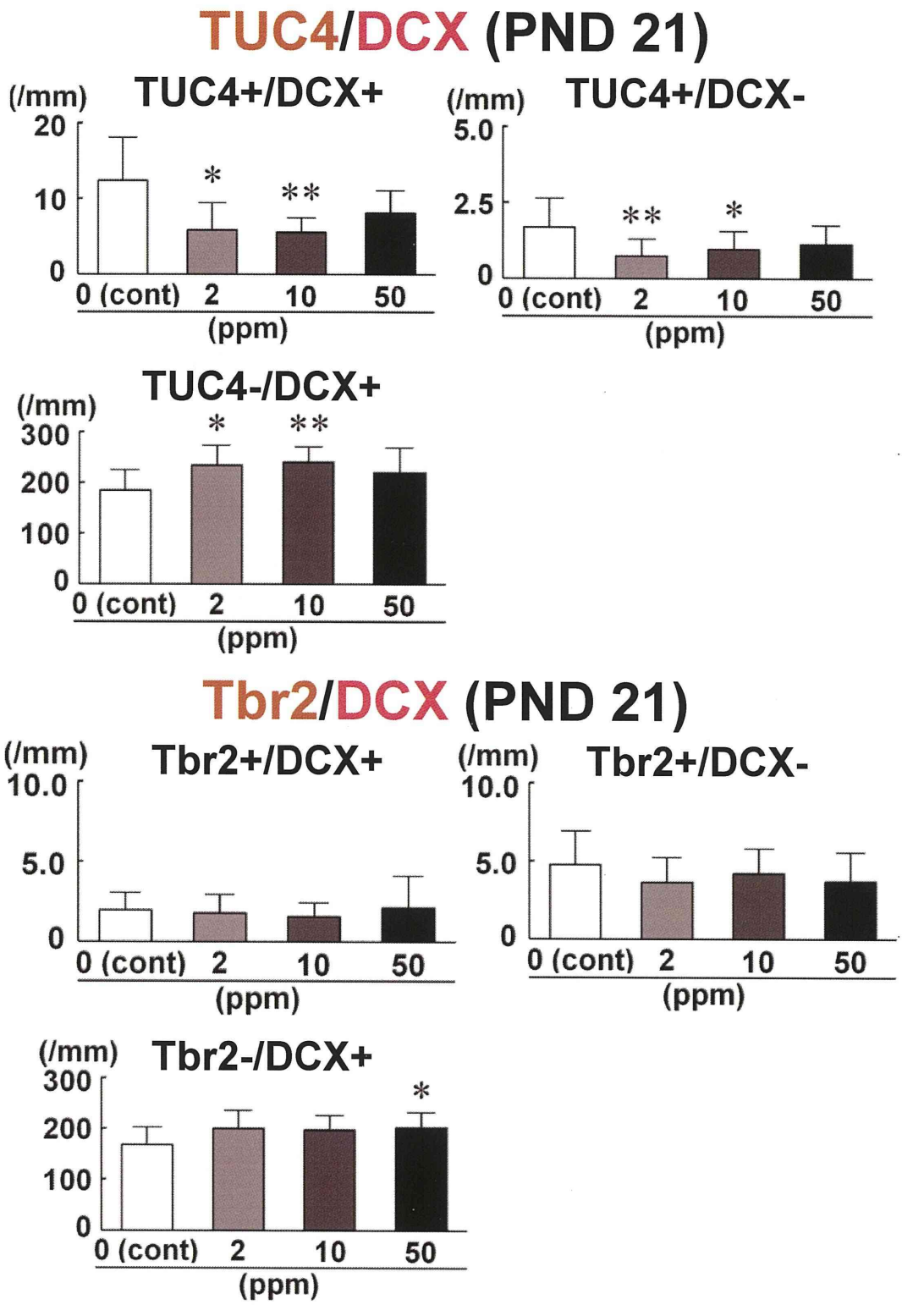

Fig. 37. Distribution of immunoreactive cells by double staining for DCX and TUC4 or Tbr2 in the dentate subgranular zone of male offspring at PND 21 after maternal exposure to nicotine hydrogen tartrate salt from GD 6 to PND 21 in rats.

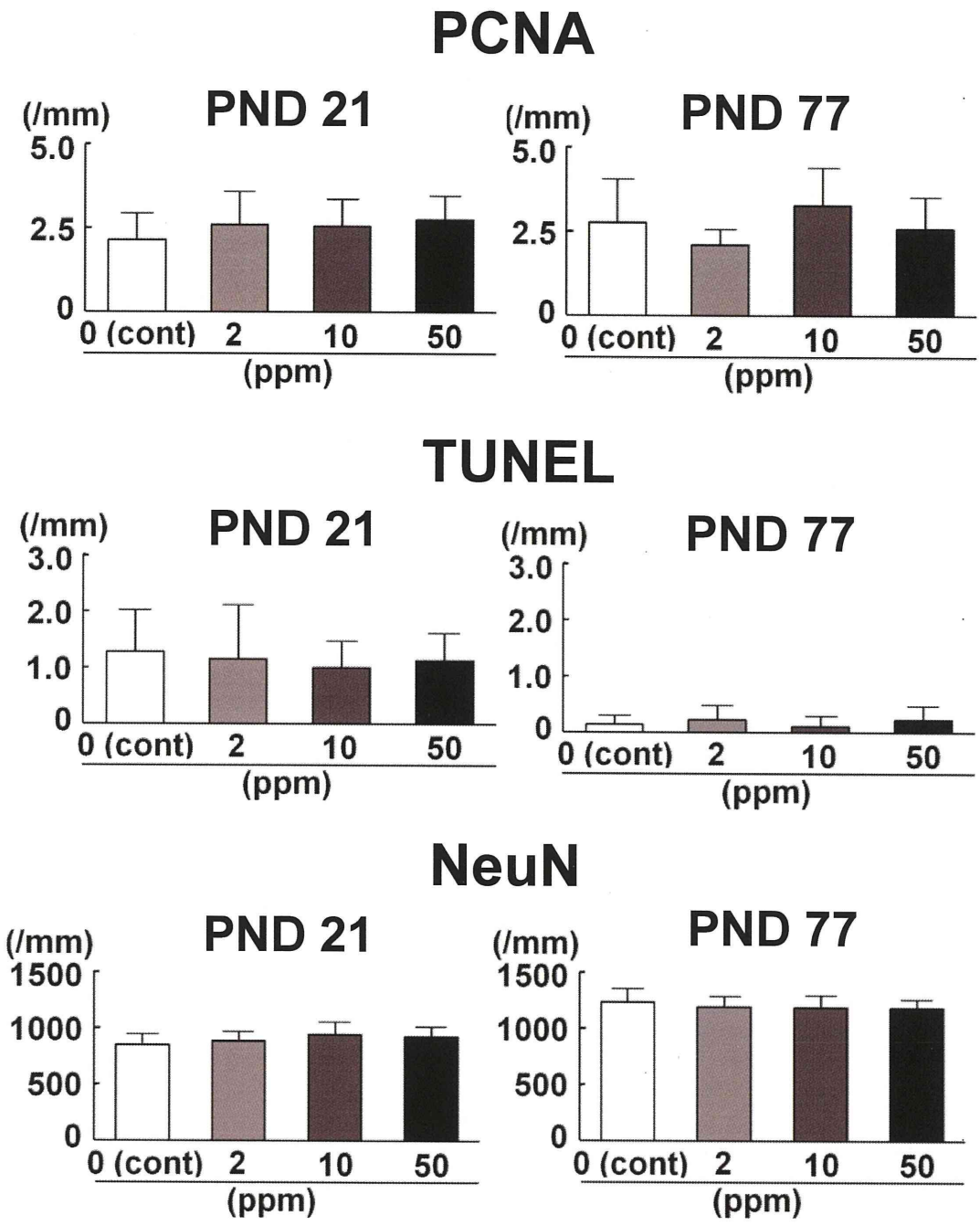

Fig. 38. Distribution of TUNEL-positive apoptotic cells and PCNA-positive proliferating cells in the dentate subgranular zone and NeuN-positive post mitotic granule cells in granular cell layer of male offspring at PND 21 and 77 after maternal exposure to nicotine hydrogen tartrate salt from GD 6 to PND 21 in rats.

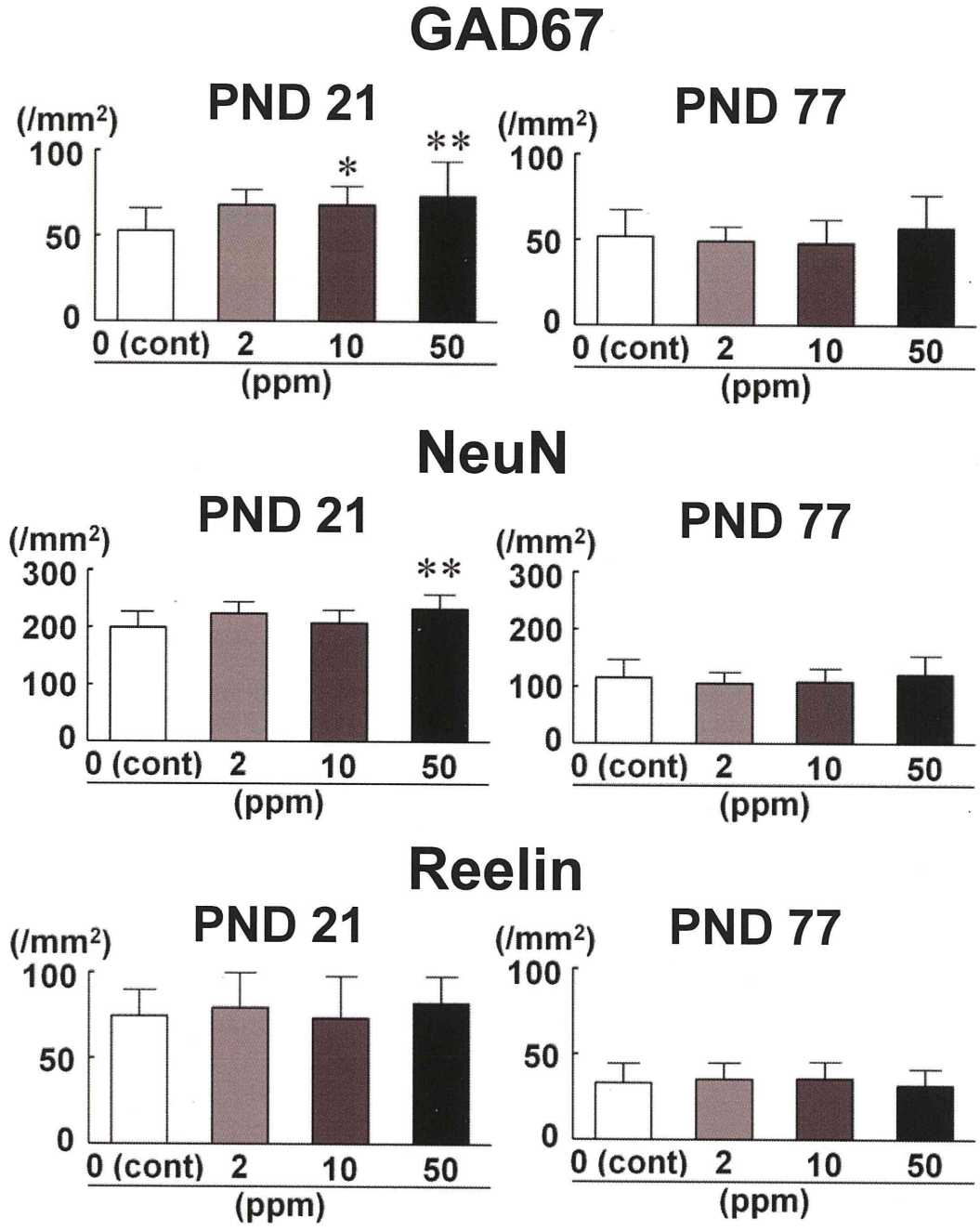

Fig. 39. Distribution of immunoreactive cells for GAD67, NeuN and reelin in the hilus of the hippocampal dentate gyrus in male offspring at PND 21 and 77 after maternal exposure to nicotine hydrogen tartrate salt from GD 6 to PND 21 in rats.

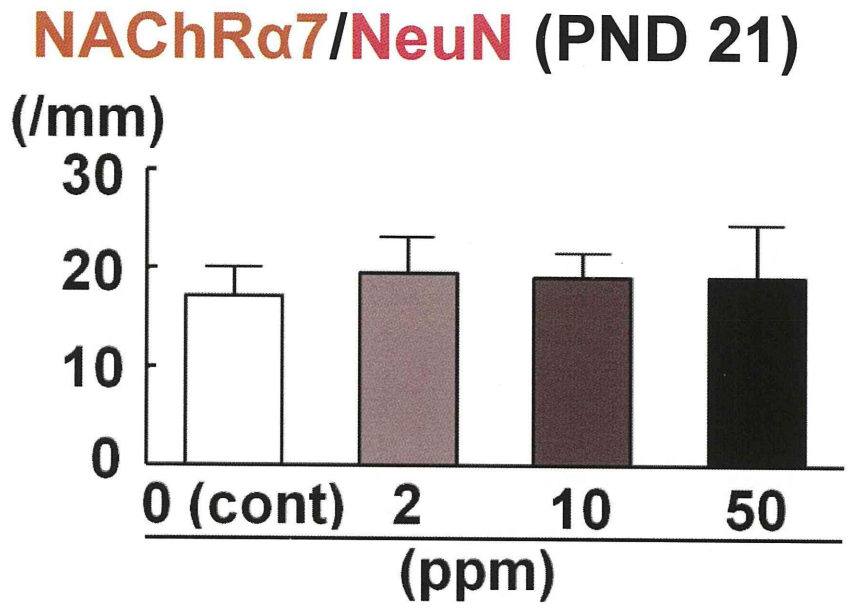

Fig. 40. Distribution of NAChRα7-positive and NeuN-negative cells by double staining in the dentate subgranular zone of male offspring at PND 21 after maternal exposure to nicotine hydrogen tartrate salt from GD 6 to PND 21 in rats.

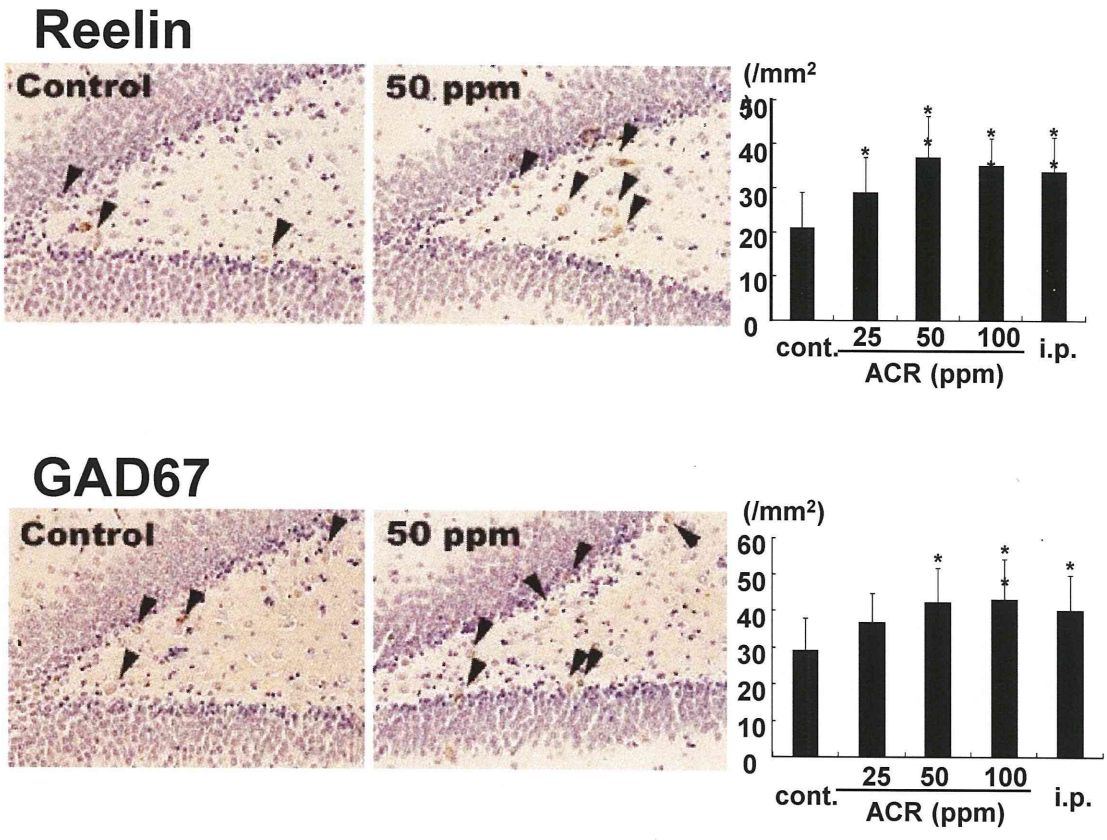

Fig. 41. Distribution of Reelin- or GAD67-immunoreactive cells in the hilus of the hippocampal dentate hilus in offspring at PND 20 after maternal exposure to acrylamide from GD 6 to PND 20 in mice. Combined data of males and females.

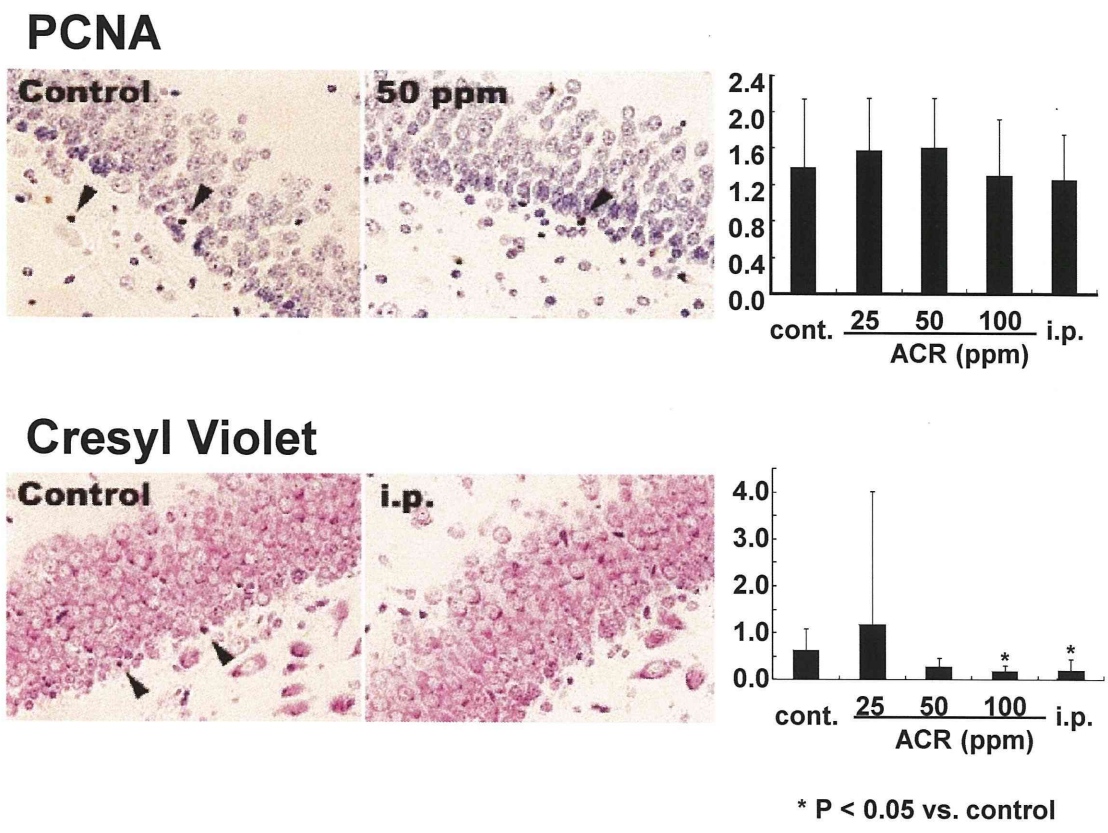

Fig. 42. Distribution of proliferating cells and apoptotic cells in the dentate subgranular zone of offspring at PND 20 after maternal exposure to acrylamide from GD 6 to PND 20 in mice. Combined data of males and females.

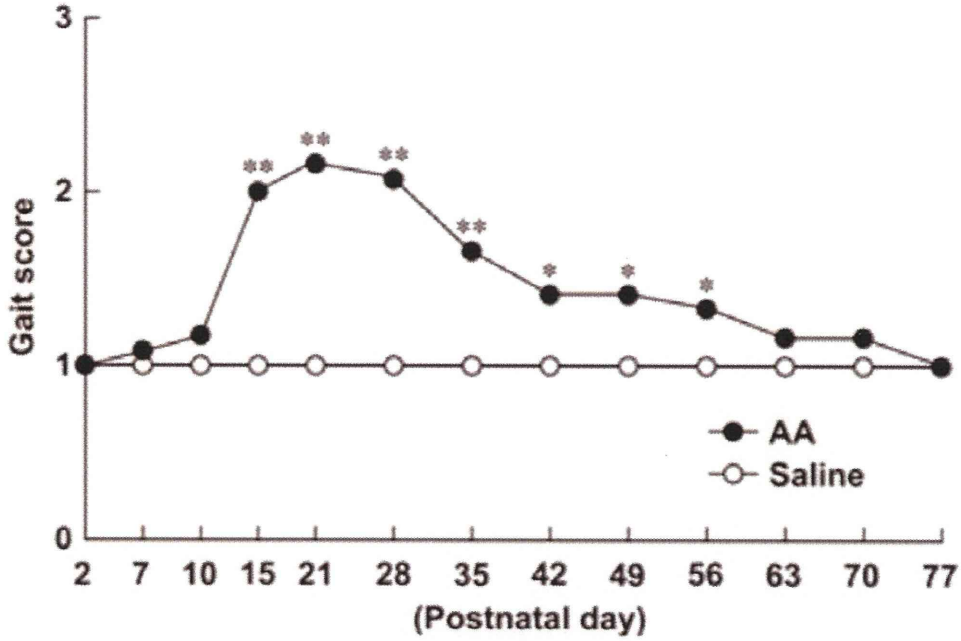

Fig. 43. Change of the average of gait score of offspring from PND2 to PND77 in Experiment 2 of the acrylamide study.

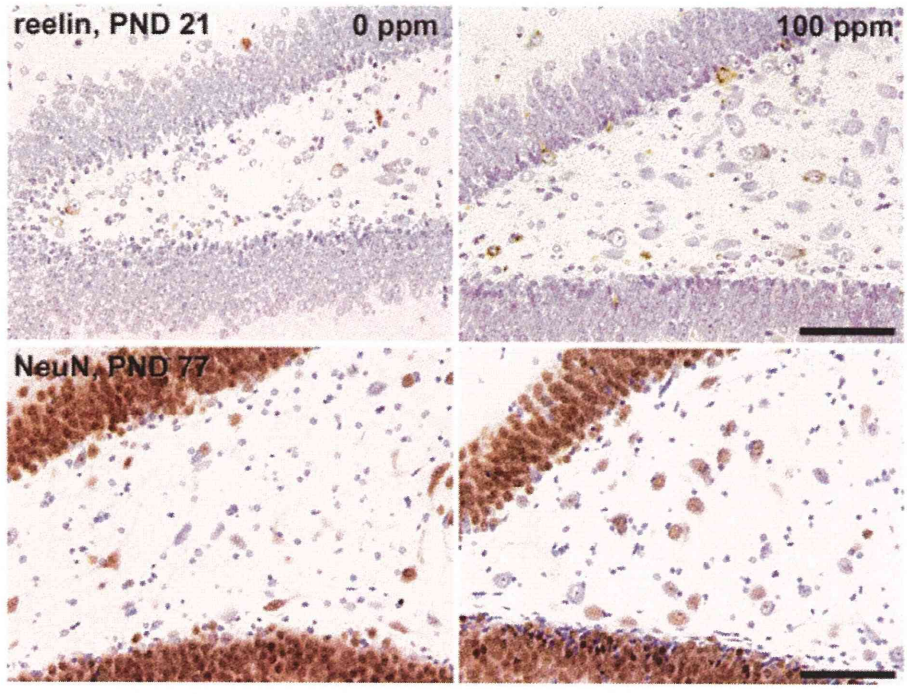

Fig. 44. Distribution of reelin- and NeuN-immunoreactive cells in the dentate hilus of pups at PND 21 and PND 77 in Experiment 1 of the acrylamide study.